Open Access Journal

Journal of Sustainable Research in Engineering 1 (3) 2014, 1-9

Journal homepage: www.jkuat-sri.com/ojs/index.php/sri/index

Performance Analysis of a Direct Drive Permanent Magnet Generator for Small Wind Energy Applications

Philip Oketch Akello[1*], Francis Xavier Ochieng[1] and Joseph Ngugi Kamau[2]

[1]*Institute of Energy and Environmental Technology, Jomo Kenyatta University of Agriculture and Technology P.O. Box 62000 – 00200, Nairobi, Kenya*

[2]*Department of Physics, Jomo Kenyatta University of Agriculture and Technology P.O. Box 62000 – 00200, Nairobi, Kenya*

[*]*Corresponding Author - E-mail: philipodhis@gmail.com*

Abstract – This paper describes performance analysis of a direct drive Axial Flux Permanent Magnet (AFPM) generator developed for small scale wind energy applications. The design process approach began by a field survey intended to understand reasons behind low penetration of Small Wind Turbines (SWTs) in Kenya and failures of existing power transmission systems, before making a decision on the most suitable electrical generator system. The main objective of this study was to design a generator that is cost efficient to improve its adoption, easy to manufacture so that it can be made in small workshops using basic tools and with limited electrical engineering knowledge, to make it attractive as a source of employment for the youth. Starting by elimination among different possible generator structures, a decision was made for the configuration of a core-less (air-cored) double rotor AFPM generator oriented to SWT applications. The design process combines both analytic and Finite Element Analysis (FEA) of the generator. A simple analytic electromagnetic design model, including sizing equations, considering the fundamental laws governing this type of machine was used to achieve and implement a prototype. FEA model and performance equations were used to verify its performance. The generator assembly is reinforced using an innovative strong T-frame to improve generator stability since coreless AFPMs are known to have stability problems. This frame provides a strong reinforcement to the generator assembly and also offers a flexible mounting support to the turbine blades so that the generator can easily be mounted both on a Horizontal Axis Wind Turbine (HAWT) as well as a Vertical Axis Wind Turbine (VAWT). The AFPM generator will be fitted with suitable protective cover to shield the generator from effects of drought such as corrosion and keep debris from becoming lodged in the inner parts. This has the possibility of extending the life of the generator. The generator has also been designed with large number of poles to improve its performance at low wind speeds. The generator efficiency is high with typical efficiency values of between 75-89%.

Keywords: Axial Flux Permanent Magnet (AFPM) Generator, Small Wind Turbine (SWT), Finite Element Analysis (FEA).

1. Introduction

Small Wind Turbines (SWTs) have been available in Kenya for more than 10 years. However, despite the huge potential for SWTs alongside the high demand for rural electricity, the pace of adoption in many rural areas is still low [1]. A major reason for the continued low penetration is the high cost of the technology particularly the drive train (gearbox and/or generator). Small scale wind power applications require a cost effective and mechanically simple drive train in order to be a reliable energy source [2]. A study has shown that the gearbox is the part in a wind turbine responsible for most downtime due to failures [3]. Consequently, most SWTs are directly connected to the generator in order to avoid the failures associated with the use of a gearbox transmission system.

The requirements of the desired generator configuration were specified based on the analysis of different SWT generator topologies and on the research objectives. Among the requirements were that the generator design should be mechanically simple for ease of manufacture and maintenance even by those with basic technical skills. The generator must also be cheap to make and easily integrated into the turbine system. In addition it should be efficient, perform well under low wind speeds and produce no cogging torque to avoid any self-starting issues associated with some types of wind turbine.

One generator that meets all these criteria is the AFPM generator with air-cored stator. This type of generator was successfully developed using locally available materials and its performance tested at a JKUAT lab. This paper provides an analysis of the generator performance.

2. Theory

2.1 Generator Topology

The AFPM generator is a machine producing magnetic flux in the axial direction with permanent magnets (PMs), Fig. 1.The generator consists of two rotor discs mounted either side of a non-magnetic, non-conducting stator. The axially magnetized PMs are embedded onto the inner surfaces of the rotor disks using polyester casting, which supports them, and also protects them from corrosion, a potential problem with Neodymium Iron Boron (NdFeB) magnets [4]. The windings are placed in the air-gap in between the rotor disks and epoxy encapsulated. The coil centres are on the same diameter circle as the magnet centres. In this type of machine, coils of wire are held steady, while the magnets spin past on the rotors. Because the magnets are arranged N-S-N-S, the direction of the field flips each time a magnet goes by. Each coil encounters a flipped magnetic field, and pulse of electricity is produced, according to Faraday's law of electromagnetic induction. Although generators can readily be designed for any number of phases the generator described in this paper is a three phase machine with 12 magnets per disc and 9 stator coils. Fig. 2 shows pictures of finished stator and rotor disks before assembling while Fig. 3 is the complete double-rotor AFPM generator with air-cored stator assembled for this research.

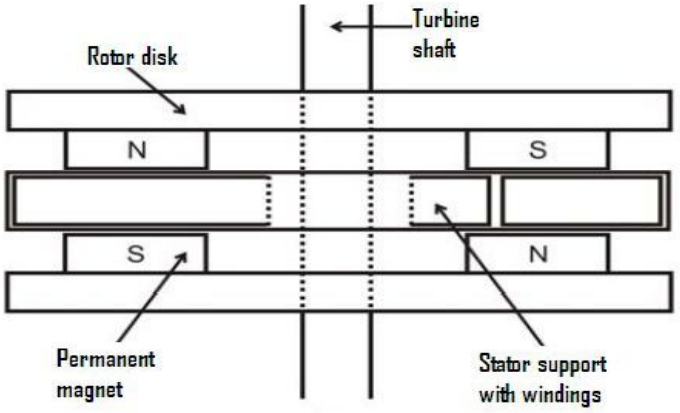

Fig. 1. Structure of the double-rotor axial flux machine with air cored stator [5].

2.2 Generator Parameters

There are many unknown parameters concerning the design of a PM machine, and to simplify the design process, it is necessary to fix some of them. Actual generator design starts with the determination of the main dimensions. The equations of dimensions used for the design of the AFPM generator are presented in Appendix 1. The fixed generator parameters and calculated dimensions are summarized in Table 1.

(a) (b)

Fig. 2. (a) Stator mould; (b) Rotor disks with PMs

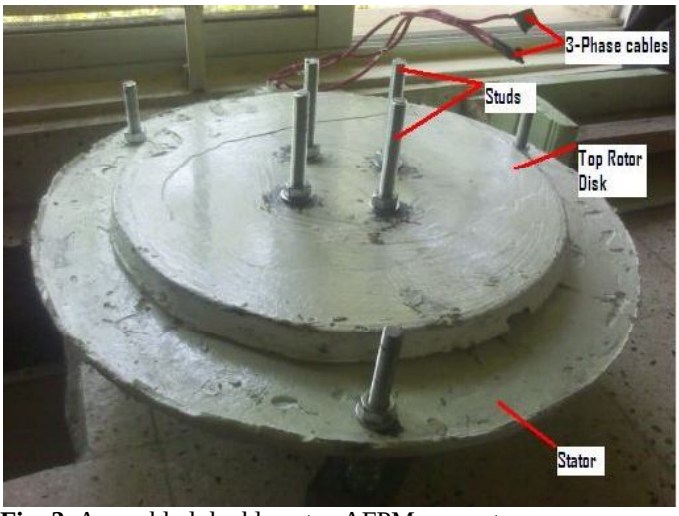

Fig. 3. Assembled double-rotor AFPM generator

Table 1: Generator main parameters

Symbol	Quantity	Value
P_{out}	Output power	1kW
N	Rated speed	500RPM
V	Output voltage	24V
P	Number of pole pairs	12
Φ	Phase number	3
ri	Inner rotor disk radius	129mm
ro	Outer rotor disk radius	175mm
Dr	Rotor diameter	350mm
rsi	Inner stator radius	129mm
rso	Outer stator radius	240mm
ts	Stator thickness	10mm

2.1 Performance Equations

The steady-state performance of AFPM generator is calculated with the use of an equivalent circuit in generator mode [5] as shown in Fig. 4 [8]. The induced electro-motive force (EMF) is represented by generator ac-voltage source E_{gen}, connected in parallel with a resistor, R_{eddy}, which models the eddy current losses in the stator. These are in turn connected in series to a resistor, R_i and an inductor L_i, representing the internal impedance of the generator. The resultant current, I_{ac}, is chosen as flowing out of generator model, while voltage measured across generator terminals is V_{gen}.

2.1.1 Induced Phase Voltage

The Root Mean Square (RMS) value of sinusoidal phase voltage of non-overlapping winding of AFPM generator is given by [8]

$$E_{ph} = \frac{q}{a}\frac{2\sqrt{2}}{p}\omega B_p N_t r_e l_a k_p k_d \quad (1)$$

where q is the number of stator coils per phase, a is the number of parallel connected circuits, p is the number of poles, ω is the generator rotating speed (rad/s), B_p is the peak air-gap flux density, N_t is the number of turns per coil, r_e is average radius of stator winding, l_a is active length of stator winding, k_p is pitch factor of non-overlapping winding and k_d is the distribution factor.

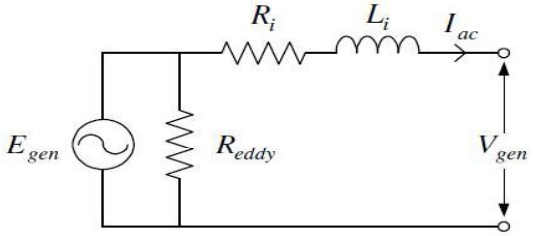

Fig. 4. Equivalent circuit of an AFPM Generator [6]

The peak value of air-gap flux density, B_p, can be calculated as

$$B_p = (2\sqrt{3}B_g)/\pi \quad (2)$$

where B_g is the flux density waveform in the air-gap.

$$r_e = (r_i + r_o)/2 \quad (3)$$

where r_i and r_o are the inner and outer radii of the stator respectively.

$$l_a = r_o - r_i \quad (4)$$

$$k_p = \frac{sin(\theta_m[1-k]/2)\, sin(k\theta_m/2)}{(k\theta_m/2)} \quad (5)$$

$$\theta_m = \pi p/Q \quad (6)$$

where Q is the total number of stator coils

$$k = \theta_{re}/\theta_m \quad (7)$$

$$\theta_{re} = \frac{\pi}{3}\left(\frac{r_i - l_g}{r_e}\right) \quad (8)$$

$$k_d = \frac{sin(n[\theta_m - \pi]/2)}{n\, sin([\theta_m - \pi]/2)} \quad (9)$$

2.1.2 Stator Phase Resistance

The per-phase resistance, R_{ph}, of stator windings is the sum of internal resistances, R_i, of each coil in a phase which can be obtained by:

$$R_i = \rho_{cu} L/A \quad (10)$$

where ρ_{cu} is the resistivity of copper wire used, L is the length of wire per coil and A is the cross-sectional area of the wire chosen. Therefore,

$$R_{ph} = 3R_i \quad (11)$$

The generator power output per phase can be obtained from the following equation:

$$P_{ph} = V_o^2/(4R_{ph}) \quad (12)$$

where V_o is the open circuit phase voltage. The generator power output, P_{out} is the sum of power outputs from each phase.

2.1.3 Stator Inductance

The AFPM generator utilizes a coreless stator which results in low internal inductance. The inductance of the stator winding can be calculated as follows [9]

$$L = \left[\frac{q(2l_a+l_e)^2 N_t^2}{h_a}\right] 10^{-7} K_n \quad (13)$$

where h is axial height of coil, l_e end winding length of coil and K_n Nagaoka constant. End-winding length of coil is obtained by [8]

$$l_e = 2\theta_m(r_o + r_i)\frac{1-0.6k}{p} \quad (14)$$

Nagaoka constant, K_n is given by [10]

$$K_n = \frac{1}{1+0.9\left(\frac{2l_a+l_e}{2\pi h_a}\right)+0.32\left(\frac{2\pi w_{cs}}{2l_a+l_e}\right)+0.84\left(\frac{w_{cs}}{h_a}\right)} \quad (15)$$

where w is width of coil side as indicated in Fig. 5.

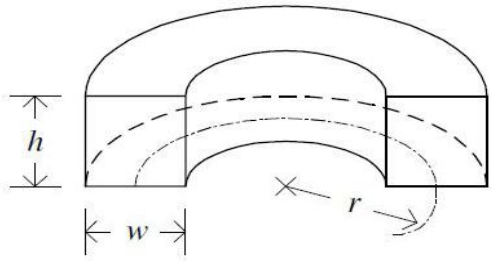

Fig. 5. Cross-section of round estimation of stator coil [7]

2.1.4 Types of Losses in the Generator

The machine no-load loss consists of loss components in both stator (copper and eddy current losses) and rotor disks (windage and bearing/frictional losses).

Per-phase copper losses are calculated by

$$P_{cu} = 3I_{ph}^2 R_{ph} \quad (16)$$

where I_{ph} is the RMS value of EMF voltage of stator phase winding calculated as follows [5]

$$I_{ph} = \frac{\sqrt{2}}{2} k_w N_s \omega B_p (r_{so}^2 - r_{si}^2) \quad (17)$$

where N_s is the number turns of a stator phase and k_w the winding factor which is a product of k_p and k_d described earlier.

Stator eddy current losses equation is given by Carter [9]

$$P_{eddy} = \frac{1}{32}(\omega B_p d)^2 \left(\frac{2N_t l_a}{\rho_{cu}}\right)\left(\frac{\pi d^2}{4}\right) \quad (18)$$

where d is wire diameter.

The mechanical/rotational loss (which includes windage and frictional/bearing losses) is estimated from the following equation [11]

$$P_{mech} = \frac{1}{2} C_f \rho_r (\pi\omega^3)(D_{ro}^5 - D_{ri}^5) \quad (19)$$

where ρ_r is density of rotating part, D_{ro} and D_{ri} are outer and inner diameters of stator respectively. C_f is friction coefficient calculated as follows [13]

$$C_f = \frac{3.87}{\sqrt{R_e}} \quad (20)$$

where R_e is Reynolds number for outer radius of the machine given by

$$R_e = (\omega \rho_r r_o^2)/\mu \quad (21)$$

where μ is the kinematic viscosity of air.

2.1.5 Generator Efficiency

The total electromechanical efficiency of the generator is given by

$$\eta = \frac{P_{out}}{P_{in}} \times 100\% \quad (22)$$

where P_{out} and P_{in} are generator power output and power input respectively. Power input is obtained by

$$P_{in} = P_{out} + P_{loss} \quad (23)$$

$$P_{loss} = P_{cu} + P_{eddy} + P_{mech} \quad (24)$$

3. Results and Analysis

3.1 Finite Element Magnetic (FEM) Analysis

The Finite Element Analysis (FEA) is a flexible, reliable and effective method for the analysis and synthesis of power-frequency electromagnetic and electromechanical devices [13]. Finite Element Magnet Method (FEMM 4.2) software [14] was used. It is a suite of programs for solving low frequency electromagnetic problems on two-dimensional planar and axisymmetric domains.

The calculated and FEMM analyzed values for both phase resistance and inductance of the generator were compared. This is done to check for any significant inconsistencies that might occur in the fabrication of the

generator [5]. Significant differences of more than 5% or large differences between phases may indicate a fabrication error. Both calculated and FEMM analysis results are provided in Table 2 below, and they show maximum difference of less than 5%.

Table 2: Resistance and inductance results

Parameter	Sizing Equation	FEMM Value	%Variation
Resistance	0.8271 Ω	0.8595 Ω	3.8
Inductance	0.9440 mH	0.9120mH	3.5

3.2 Generator Test Set-up

Tests were conducted to determine generator open circuit (no-load) performance and rectified DC voltage characteristics. The no-load test set-up consists of a Variable Speed Drive (VSD) controlling the power to a 3-phase motor. The motor is used as a prime mover emulating the mechanical characteristics of a wind turbine. The VSD measures the input frequency (hence speed in RPM) into the generator. A multi-meter is used to measure line ac-voltages. Fig. 6 shows the generator connected to the motor and VSD. After completing the no-load tests, the 3 phase generator AC output is now rectified through a power control unit and the resultant DC output characteristics determined. Measurements and performance calculations are presented as Appendix 2.

The control unit (Fig. 7) consists of a break switch, bridge rectifier, charge controller, dump load and fuse (circuit breaker). The brake switch is a useful feature for stopping the wind turbine if necessary. The diodes in the bridge rectifier ensure that current will only flow one way into the battery and cannot discharge it. The disadvantage of diodes is that there is a large drop of voltage across them at all times when they are operating [4].

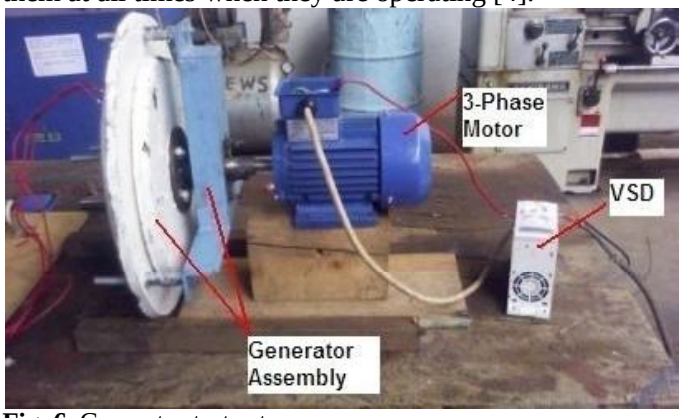

Fig. 6. Generator test set-up

All the positive terminals are connected to battery positive via the fuse or circuit breaker while all the negative terminals are connected to the battery negative.

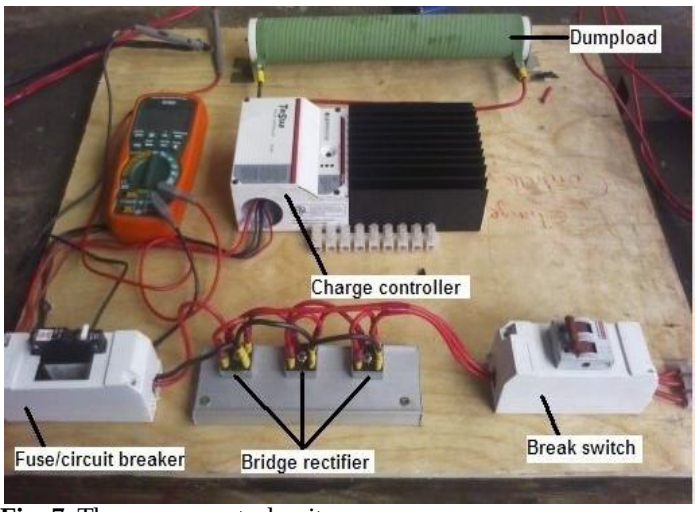

Fig. 7. The power control unit

The AFPM generator is connected to the control unit via the break switch.

3.3 Analysis of Generator Performance

The calculated results in Appendix 2 are used to analyse the generator performance.

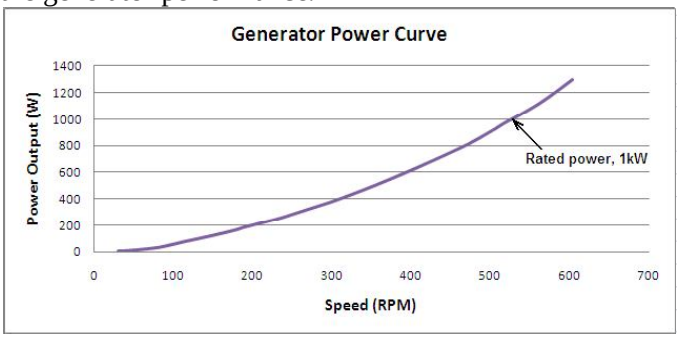

Fig. 8. Generator output power curve

Fig. 8 shows generator power curve indicating good power production characteristics. Power output increases with increase in generator speed and goes beyond the rated power of 1 kW before it is expected to level off at a certain maximum speed. The power output did not peak because the generator was not tested beyond 600 rpm. Since SWTs usually operate under relatively low wind speed regimes, power production at lower speeds is much more crucial to take into account.

At rated speed, mechanical losses account for 92% of total losses. These losses are brought about by the car hub bearing and the weight of rotor disks used. The no-load losses characteristics graph is shown in Fig. 9 below.

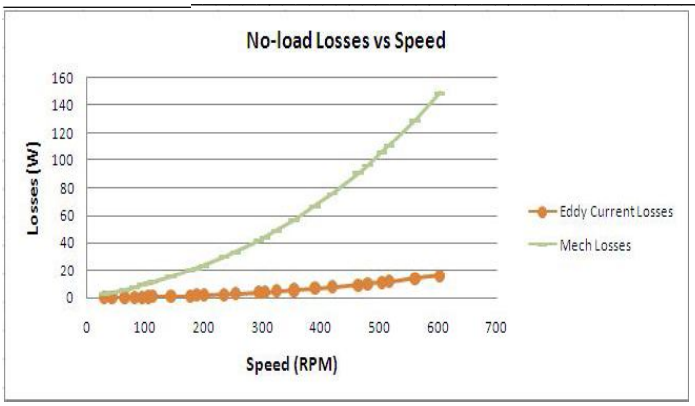

Fig. 9. Generator losses at various speeds

The use of a more efficient bearing and lighter rotor disks can reduce mechanical losses and increase efficiency. The loss contribution due to stator eddy current was 3W (8% of total losses) at rated speed. Using wire with smaller diameter can minimize the losses which vary with the diameter of stator conductor to the fourth power (equation 18).

The generator attains maximum efficiency of 87% at rated speed and beyond. This efficiency is acceptable as high for a non-optimized prototype [2]. Fig. 10 is the generator efficiency curve.

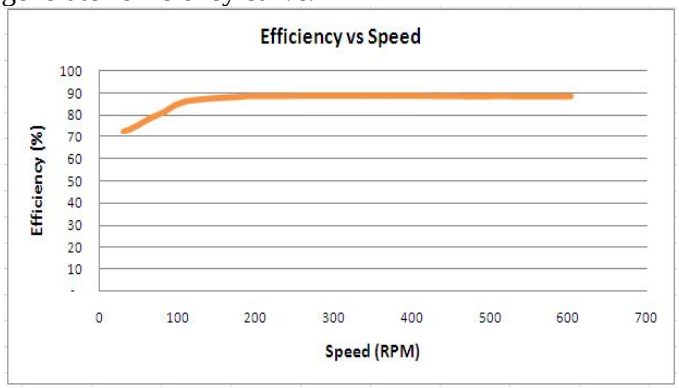

Fig. 10. Generator efficiency versus Speed

Finally, the rectified DC voltage characteristics were analyzed from Fig. 11 to determine the generator cut-in speed for battery charging. The generator was designed for charging a 24V battery charging system and the cut-in speed determined at the point where rectified DC voltage equals 24VDC. At 24VDC, the generator cut-in speed for battery charging is found to be 153.69 rpm, equivalent to a wind speed of 2.82m/s. This is suitable for SWT applications where low and medium wind speeds are predominant, like in most off-grid regions in Kenya.

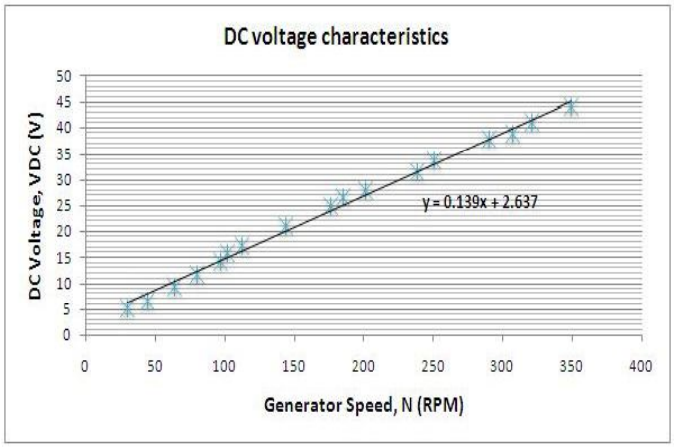

Fig. 11. Rectified DC voltage characteristics

4. Conclusions

The analysis of AFPM generator performance has been presented. The fabrication process met design specifications and this is verified by the analysis of FEA and sizing equations. The generator fabrication process is also short and simple, and this can be accomplished in a small workshop using basic tools. The generator cut-in speed for battery charging is about 154 rpm. This is equivalent to a wind speed of 2.8 m/s. The AFPM generator is therefore expected to perform well under low wind speed conditions. The generator attains maximum efficiency (about 89%) at low speeds which is suitable for SWT applications where low and medium wind speeds are predominant and high wind speeds are rare. Since mechanical losses vary with coefficient of bearing friction and rotor diameter to the fifth power (equation 19), the use of a more efficient bearing and rotor disk with reduced outer diameter will minimize these losses and increase generator efficiency. Eddy current losses can also be minimized further by using winding wire of smaller diameter.

Acknowledgements

The authors acknowledge the Kenya National Commission for Science, Technology and Innovation (NACOSTI) for funding this research.

References

[1] Vanheule, L, “Small Wind Turbines in Kenya, An analysis with Strategic Niche Management”, Delft University of Technology, Delft, Netherlands: Master Thesis, 2012.

[2] A. Ferreira, A. Silva, and A. Costa, "Prototype of an Axial Flux Permanent Magnet Generator for Wind Energy Systems Applications," in *12th European Conference on Power Electronics and Applications, EPE 2007*, Aalborg, Denmark, 2007.

[3] J. Ribrant and L.M. Bertling, L.M, “Survey of failures in wind power systems with focus on Swedish wind power plants during 1997-2005,” *IEEE Transactions on Energy Conversion*, vol. 22(1), 2007, pp. 167-173.

[4] H. Piggott, "Permanent magnet alternator theory session for ITDG wind power course," Hambantota, Sri Lanka, 2003.
[5] S.O. Ani, *Low Cost Small Wind Turbine Generators for Developing Countries*. The Netherlands: Wöhrmann Print Service, Zutphen, 2013.
[6] F.G. Rossouw , "Analysis and design of axial flux permanent magnet wind generator system for direct battery charging applications," Stellenbosch University, Matieland, South Africa, May 2009.
[7] R. Wang, "Design aspects and optimization of an axial field permanent magnet machine with an ironless stator," Ph.D. dissertation, University of Stellenbosch, 2003.
[8] M.Kamper, R. Wang, and F. Rossouw, "Analysis and performance of axial flux permanent magnet machine with air-cored non-overlapping concentrated stator windings," in *IAS*, 2008.
[9] V.G. Welsby, *The theory and design of inductance coils*. MacDonald & Co, 1950.
[10] G.W. Carter, *The Electromagnetic Field in its Engineering Aspects*, 2nd ed. London:Longmans, 1967.
[11] J. Saari, "Thermal analysis of high-speed induction machines," Ph.D. dissertation, Helsinki Univ. Technology, Helsinki, Finland, January 1998.
[12] L. Nasrin, "Improved version of energy efficient motor for Shell Eco marathon," Royal Institute of Technology, Stockholm, Sweden, 2011.
[13] P. Gottipati, "Comparative study on double-rotor brushless motors with cylindrical and disc type slot-less stator," M.S. Thesis, Louisiana State University, USA, August 2007.
[14] *Finite Element Magnets Method*, FEMM 4.2. (2013). Available: www.femm.info/wiki/Downl
[15] Bang, D.J., Polinder, H., Shrestha, G., and Ferreira, J.A, "Review of generator systems for direct-drive wind turbines". Proceedings of the European Wind Energy Conference (EWEC) and Exhibition, Brussels, Belgium, 2008, pp. 1-11.

APPENDIX 1: Design Calculations

INITIAL DATA	DESIGN CALCULATIONS	RESULTS
	Dimensions of the Magnet Magnet Length, l_m = 46mm Magnet Width, w_m = 30mm Magnet Thickness, h_m = 10mm	**l_m = 46mm** **w_m = 30mm** **h_m = 10mm**
	Ratio of Inner to Outer Stator Radius, (λ) r_i = 129mm r_o = 175mm λ = 129/175 = 0.74	**λ = 0.74** **r_i = 129mm** **r_o = 175mm**
r_o = 175mm	**Diameter of the Machine, (D)** $D = 2\ r_o$ = 350mm	**D = 350mm**
h_m = 10mm	**Axial Length of the Stator, (L_s)** $L_s = t_w = h_m$ = 10mm	**L_s = 10mm**
	Rotor Disk Thickness, (h_r) A thickness of 10mm was adopted. Therefore, h_r = 10mm	**h_r = 10mm**
h_r = 10mm *h_m = 10mm*	**Axial Length of the Rotor, (L_r)** $L_r = h_r + h_m$ = 10 + 10 L_r = 20mm	**L_r = 20mm**
r_o = 175mm *r_i = 129mm*	**Average Air-gap Diameter of the Machine, (D_g)** $D_g = r_o + r_i$	**D_g = 304mm**

	= 175 + 129 D_g = 304mm	
g = 1.5mm *h_m = 10mm* *t_w = 10mm*	**Effective Air-gap, (g_e)** Airgap,*g* used was 1.5mm $g_e = 2h_m + 2g + t_w$ = 20 + 3 + 10 g_e = 33mm	**g_e = 33mm**
L_r = 20mm *L_s = 10mm*	**Axial Length of the Machine, (L_g)** $L_g = 2L_r + L_s + 2g$ L_g = 40 + 10 + 3	**L_g = 53mm**
p = 12	**Average Pole Pitch, τ_p** $\tau_p = \pi D_g/p$ = 0.304π/12 τ_p = 0.08	**τ_p = 0.08**
p = 12	**Number of Stator Coils, (Q)** $Q = \frac{3}{4} x\ p$ Q = 9	**Q = 9**
V= 24V *P = 1000W* *ρ_{cu} = 1.68x10^{-8} Ωm* *C_c = 0.21m*	**Number of Turns per Coil, (N_c)** $N_c = \frac{AV^2}{3C_c\rho_{cu}P}$ =π(0.8x10^{-3})^{2}x24^2/3x0.21x1.68x10^{-8}x1000 = 109.42	**N_c= 110 turns**
For N40 NdFeB magnet, *B_r = 1.29T* *(Appendix D)*	**Flux Density in the Air-gap, (B_g)** $B_g = \frac{B_r h_m}{h_m + g + t_w}$ = 1.29x0.01/(0.01+0.0015+0.01 = 0.6T	**B_g = 0.6T**

Appendix 2: No-load Measurement and Calculation Results

N (rpm)	ω (rad/s)	V_{oc} (V)	P_{ph} (W)	P_{out} (W)	P_{cu} (W) x10^{-4}	P_{eddy} (W)	P_{fr} (W)	P_{wind} (W)	P_{loss} (W)	P_{in} (W)	P_{out}/ P_{in}	η (%)
30	3.15	2.81	2	7	0.05	0.04	2.65	0.05	3	10	0.72	72
43	4.52	3.57	4	11	0.08	0.08	3.79	0.13	4	15	0.74	74
65	6.83	5.06	8	23	0.10	0.19	5.73	0.37	6	29	0.79	79
82	8.61	6.29	12	36	0.21	0.30	7.23	0.65	8	44	0.81	81
95	9.98	7.63	17	52	0.48	0.40	8.38	0.94	10	62	0.84	84

105	11.03	8.56	22	66	0.77	0.49	9.26	1.21	11	77	0.86	86
113	11.87	9.26	26	77	1.03	0.56	9.97	1.45	12	89	0.87	87
144	15.12	11.40	39	117	1.26	0.91	12.70	2.67	16	133	0.88	88
177	18.59	13.47	54	163	1.46	1.38	15.61	4.47	21	185	0.88	88
188	19.74	14.30	61	184	2.38	1.56	16.58	5.19	23	207	0.89	89
200	21.00	15.01	68	203	3.59	1.76	17.64	6.06	25	228	0.89	89
235	24.68	16.89	86	257	4.05	2.44	20.73	9.07	32	289	0.89	89
250	26.25	18.05	98	293	4.59	2.76	22.05	10.59	35	329	0.89	89
294	30.87	20.25	123	369	6.33	3.81	25.93	15.88	46	415	0.89	89
305	32.03	20.86	131	392	7.16	4.10	26.90	17.41	48	440	0.89	89
325	34.13	22.00	145	436	9.91	4.66	28.67	20.41	54	489	0.89	89
354	37.17	23.63	168	503	10.66	5.53	31.22	25.27	62	565	0.89	89
390	40.95	25.65	197	592	12.11	6.71	34.40	32.19	73	665	0.89	89
420	44.10	27.28	223	670	14.37	7.78	37.04	38.75	84	753	0.89	89
464	48.72	29.62	263	790	17.44	9.49	40.92	49.70	100	890	0.89	89
480	50.40	30.53	280	839	20.23	10.16	42.34	54.10	107	945	0.89	89
504	52.92	31.99	307	921	24.68	11.20	44.45	61.12	117	1,038	0.89	89
517	54.29	32.81	323	969	26.42	11.79	45.60	65.14	123	1,091	0.89	89
564	58.91	35.24	373	1097	29.12	13.88	49.48	79.89	143	1,161	0.89	89
613	63.32	37.96	432	1090	30.65	16.04	53.18	95.69	165	1,322	0.89	89